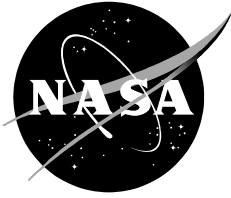


NASA/TM-2004-213155



**Deformation and Flexibility Equations
for ARIS Umbilicals Idealized as Planar Elastica**

R. David Hampton

U. S. Military Academy, West Point, New York 10996

Michael J. Leamy

University of Maine, Orono, Maine 04469

Paul J. Bryant

United Defense, Louisville, Kentucky 40214

Naveed Quraishi

Johnson Space Center, Houston, Texas 77058

The NASA Scientific and Technical Information Program Office ... in Profile

Since its founding, NASA has been dedicated to the advancement of aeronautics and space science. The NASA Scientific and Technical Information (STI) Program Office plays a key part in helping NASA maintain this important role.

The NASA STI Program Office is operated by Langley Research Center, the lead center for NASA's scientific and technical information. The NASA STI Program Office provides access to the NASA STI Database, the largest collection of aeronautical and space science STI in the world. The STI Program Office is also NASA's institutional mechanism for disseminating the results of its research and development activities. These results are published by NASA in the NASA STI Report Series, which includes the following report types:

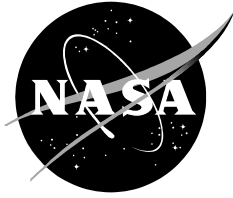
- TECHNICAL PUBLICATION. Reports of completed research or a major significant phase of research that present the results of NASA programs and include extensive data or theoretical analysis. Includes compilations of significant scientific and technical data and information deemed to be of continuing reference value. NASA counterpart of peer-reviewed formal professional papers, but having less stringent limitations on manuscript length and extent of graphic presentations.
- TECHNICAL MEMORANDUM. Scientific and technical findings that are preliminary or of specialized interest, e.g., quick release reports, working papers, and bibliographies that contain minimal annotation. Does not contain extensive analysis.
- CONTRACTOR REPORT. Scientific and technical findings by NASA-sponsored contractors and grantees.
- CONFERENCE PUBLICATION. Collected papers from scientific and technical conferences, symposia, seminars, or other meetings sponsored or co-sponsored by NASA.
- SPECIAL PUBLICATION. Scientific, technical, or historical information from NASA programs, projects, and missions, often concerned with subjects having substantial public interest.
- TECHNICAL TRANSLATION. English-language translations of foreign scientific and technical material pertinent to NASA's mission.

Specialized services that complement the STI Program Office's diverse offerings include creating custom thesauri, building customized databases, organizing and publishing research results ... even providing videos.

For more information about the NASA STI Program Office, see the following:

- Access the NASA STI Program Home Page at <http://www.sti.nasa.gov>
- E-mail your question via the Internet: help@sti.nasa.gov
- Fax your question to the NASA STI Help Desk at (301) 621-0134
- Telephone the NASA STI Help Desk at (301) 621-0390
- Write to:
NASA STI Help Desk
NASA Center for AeroSpace Information
7121 Standard Drive
Hanover, MD 21076-1320

NASA/TM-2004-213155



**Deformation and Flexibility Equations
for ARIS Umbilicals Idealized as Planar Elastica**

R. David Hampton
U. S. Military Academy

Michael J. Leamy
University of Maine

Paul J. Bryant
United Defense

Naveed Quraishi
Johnson Space Center

National Aeronautics
and Space Administration

Johnson Space Center
Houston, Texas 77058-3696

January 2005

Available from:

NASA Center for AeroSpace Information
7121 Standard Drive
Hanover, MD 21076-1320

National Technical Information Service
5285 Port Royal Road
Springfield, VA 22161

This report is also available in electronic form at <http://ston.jsc.nasa.gov/collections/TRS>

Contents	page
Abstract	ii
Nomenclature.....	iii
Introduction	1
Problem Statement	2
Equations of Umbilical Geometry.....	3
Validation (Special Cases).....	5
Equations of Umbilical Flexibility	7
Flexibility Equations.....	10
End-State Verification	11
Flexibility Verification	13
Implications for Umbilical Design	16
Conclusions	16
Appendix	17
References	19

Figures	page
1. Flexible umbilical under end loading.....	2
2. End-state and flexibilities versus load factor.....	13
3. Finite-element model of the example umbilical defined in Figure 2	15

ABSTRACT

The International Space Station relies on the active rack isolation system (ARIS) as the central component of an integrated, station-wide strategy to isolate microgravity space-science experiments. ARIS uses electromechanical actuators to isolate an international standard payload rack from disturbances due to the motion of the Space Station. Disturbances to microgravity experiments on ARIS-isolated racks are transmitted primarily via the ARIS power and vacuum umbilicals. Experimental tests indicate that these umbilicals resonate at frequencies outside the ARIS controller's bandwidth at levels of potential concern for certain microgravity experiments. Reduction in the umbilical resonant frequencies could help to address this issue.

This work documents the development and verification of equations for the in-plane deflections and flexibilities of an idealized umbilical (thin, flexible, inextensible, cantilever beam) under end-point, in-plane loading (inclined-force and moment). The effect of gravity is neglected due to the on-orbit application. The analysis assumes an initially curved (not necessarily circular), cantilevered umbilical with uniform cross-section, which undergoes large deflections with no plastic deformation, such that the umbilical slope changes monotonically. The treatment is applicable to the ARIS power and vacuum umbilicals under the indicated assumptions.

NOMENCLATURE

Lower Case

c_ξ	Cosine of umbilical angle ξ at arbitrary point R on umbilical
f, g	Arbitrary functions
s	Distance along umbilical from cantilevered end (point O)
s_ξ	Sine of umbilical angle ξ at arbitrary point R on umbilical
y	Position coordinate (for arbitrary point R on umbilical)
y_c	Position coordinate for umbilical terminus (point C)
z	Position coordinate (for arbitrary point R on umbilical)
z_c	Position coordinate for umbilical terminus (point C)
α_i	Convenience variable
β_i	Flexibility integral
ς	Initial (unloaded-umbilical) angle of tangent to umbilical at arbitrary point R
ς_c	Initial (unloaded-umbilical) angle of tangent to umbilical at terminal point C
η	Square of shape kernel
θ	Shape kernel
κ^i	Umbilical initial (unloaded) curvature
κ_c^i	Umbilical initial curvature at terminus C
λ	Load magnification factor
ξ	Final (loaded-umbilical) angle of tangent to umbilical at arbitrary point R
ξ_c	Final (loaded-umbilical) angle of tangent to umbilical at terminal point C
ρ	Circular-arc test-umbilical radius of curvature, relaxed configuration
ν	Poisson's ratio

Upper Case

C	Umbilical terminus
C_1	Integration constant
E	Young's modulus of elasticity
EI	Flexural rigidity
F	Arbitrary function
I	Area moment of inertia with respect to umbilical neutral axis
L	Umbilical length
M	Internal moment
M_x	Terminally applied moment about x -axis
O	Umbilical origin
P_z	Terminally applied force, negative z -direction
Q_y	Terminally applied force, y -direction
Q_z	Terminally applied force, z -direction
R	Arbitrary point along umbilical

INTRODUCTION

The active rack isolation system (ARIS) serves as the central component of an integrated station-wide strategy to isolate microgravity space-science experiments on the International Space Station. ARIS uses eight electromechanical actuators to isolate an international standard payload rack from disturbances due to the motion of the Space Station. The full Space Station complement of ARIS racks is currently set at five. Disturbances to microgravity experiments on ARIS-isolated racks are transmitted primarily using the (nominally 13) ARIS umbilicals, which provide power, data, vacuum, cooling, and other miscellaneous services to the experiments. The two power umbilicals and, to a lesser extent, the vacuum umbilical, serve as the primary transmission path for acceleration disturbances. Experimental tests conducted by the ARIS team¹ (December 1998) indicate that looped power umbilicals resonate at about 10 Hz; unlooped power umbilicals resonate at about 4 Hz. In either case, the ARIS controller's limited bandwidth (about 2 Hz) admits only limited active isolation at these frequencies. Reduction in the umbilical resonant frequencies could help to address this problem.

Analytical studies of the nonlinear bending and deflection of a thin, flexible, inextensible, linearly elastic, fixed-end, cantilever beam (originally horizontal) have been conducted for a variety of loading conditions, including concentrated terminal transverse (vertical) loading²⁻⁶; uniformly distributed vertical loading^{2,7-9}; uniformly distributed normal loading¹⁰; concentrated terminal inclined loading^{11,12}; multiple concentrated vertical loads¹³; concentrated terminal vertical and moment loading¹³; and heavy, rigid, end-attachment loading.¹⁴ Reference 15 provided a set of nonlinear equations for the case of a weightless flexible beam with arbitrary, discrete, in-plane loads and boundary conditions. Typical exact solutions of beam deflections involve complete and incomplete elliptic integrals (for example, Refs. 2, 4-6, 13, 14). For literature reviews, see References 16-18.

For the special case of general terminal in-plane loading, which includes both inclined-force and moment loads, in-plane flexibility (or stiffness) equations are of particular interest toward umbilical design for microgravity-isolation purposes. The equations could be used to help optimize umbilical flexibilities and resonant frequencies for microgravity applications.

This work documents the development and verification of equations for the in-plane deflections and flexibilities of an initially straight, idealized umbilical under terminal in-plane loading (inclined-force and moment).¹⁹ The effect of gravity is neglected, a reasonable approximation for an on-orbit application. The deflection and flexibility analyses are applicable to a cantilevered umbilical which, when unloaded, is curved with a monotonically changing slope. The umbilical possesses a uniform cross-section, and undergoes large deflections with no plastic deformation, such that the slope of the loaded umbilical changes monotonically. The treatment is applicable to the ARIS power and vacuum umbilicals under the indicated assumptions.

PROBLEM STATEMENT

Consider an idealized, curved umbilical of length L with endpoints O and C and arbitrary intermediate point R (Fig. 1). The umbilical is idealized in the same sense as above: it is thin, flexible, inextensible, prismatic, linearly elastic, fixed-end, and cantilevered, with equal tensile and compressive moduli of elasticity E . Let R be located at distance s along the umbilical, measured from the cantilevered end (point O), with coordinates (y, z) ; the coordinates of point C are (y_c, z_c) . The coordinates have been chosen to be consistent with the coordinate system in use for the existing analyses of ARIS, for dynamic-modeling and controller-design purposes; point O , then, is the umbilical point of attachment to the Space Station, and point C is the point of attachment to the ISPR. Initially, when the umbilical is relaxed (unloaded), let it be described by an “initial” curvature of $\kappa^i(s)$. If ζ is the angle, at R , of the tangent to the umbilical, then this initial curvature is $d\zeta/ds$. When the umbilical is under load, let the tangent at R be ξ ; and let ξ_c represent the endpoint angle, at C . Assume that ξ varies monotonically with distance s , and that the flexural rigidity EI is known.

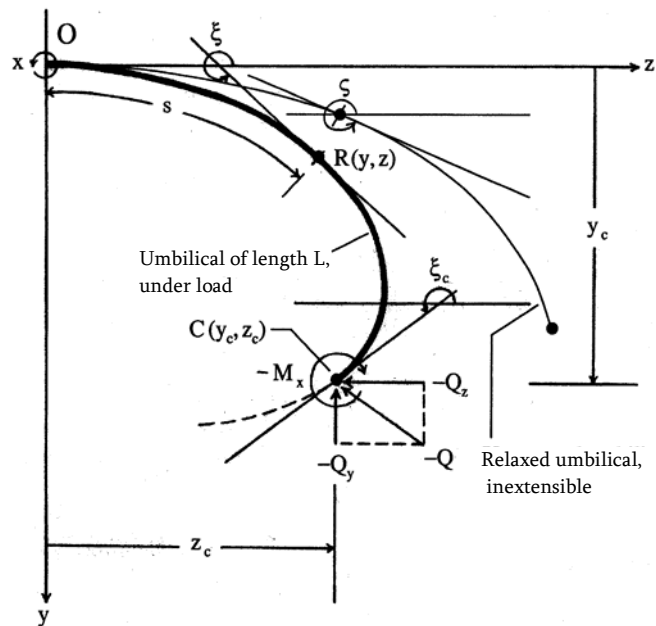


Figure 1. Flexible umbilical under end loading

This research accomplishes the following fundamental tasks: 1) to derive geometric equations for the umbilical length, coordinates at arbitrary point R , and terminal coordinates (at C); and 2) to use these equations to derive useful equations for the nine in-plane umbilical flexibilities. These 14 equations will be expressed in terms of the final slope function $\xi(s)$, the terminal angle ξ_c , the initial

(unloaded) curvature function $\kappa^i(s)$, the unloaded terminal curvature κ_c^i , and arbitrary in-plane loads at C . The loads are as follows: forces Q_y and Q_z (assumed to be positive in the positive y - and z -directions, respectively), and moment M_x (assumed to be positive in the counter-clockwise direction, about the positive x -axis).

EQUATIONS OF UMBILICAL GEOMETRY

At point R the moment equation is

$$-M = M_x + Q_z(y_c - y) - Q_y(z_c - z) = EI \left(\frac{d\xi}{ds} - \frac{d\zeta}{ds} \right). \quad (1)$$

Differentiating with respect to s , observing that

$$\frac{dy}{ds} = -\sin \xi \quad (2)$$

and

$$\frac{dz}{ds} = \cos \xi, \quad (3)$$

and using the shorthand notation $s_\xi = \sin \xi$ and $c_\xi = \cos \xi$, one obtains

$$\frac{d^2\xi}{ds^2} - \frac{d^2\zeta}{ds^2} = \frac{1}{EI} (Q_z s_\xi + Q_y c_\xi). \quad (4)$$

Integrating Equation (4) with respect to s yields

$$\frac{1}{2} \left(\frac{d\xi}{ds} \right)^2 - \frac{1}{2} \left(\frac{d\zeta}{ds} \right)^2 = \frac{1}{EI} (Q_y s_\xi - Q_z c_\xi) + C_1, \quad (5)$$

where C_1 is an integration constant. At point C , Equation (1) becomes

$$M_x = EI \left(\frac{d\xi}{ds} - \frac{d\zeta}{ds} \right) \Big|_{R \rightarrow C}, \quad (6)$$

leading to

$$\frac{d\xi}{ds} \Big|_{R \rightarrow C} = \frac{M_x}{EI} + \frac{d\zeta}{ds} \Big|_{R \rightarrow C}. \quad (7)$$

Upon applying this boundary condition to Equation (5) and rearranging, one has

$$C_1 = \frac{1}{2} \left[\left(\frac{M_x}{EI} + \frac{dc_\xi}{ds} \right)^2 - \left(\frac{dc_\xi}{ds} \right)^2 \right] \Bigg|_{R \rightarrow C} - \frac{1}{EI} (Q_y s_{\xi_c} - Q_z c_{\xi_c}), \quad (8)$$

such that Equation (5) can now be solved for $d\xi/ds$:

$$\frac{d\xi}{ds} = \pm \left\{ \frac{2}{EI} \left[Q_y (s_\xi - s_{\xi_c}) - Q_z (c_\xi - c_{\xi_c}) \right] + \left(\frac{M_x}{EI} + \kappa_c^i \right)^2 + \left[(\kappa^i)^2 - (\kappa_c^i)^2 \right] \right\}^{1/2} = \pm \eta^{1/2}, \quad (9)$$

where the radicand η is nonnegative:

$$\eta \equiv \frac{2Q_y}{EI} (s_\xi - s_{\xi_c}) - \frac{2Q_z}{EI} (c_\xi - c_{\xi_c}) + \left(\frac{M_x}{EI} + \kappa_c^i \right)^2 + (\kappa^i)^2 - (\kappa_c^i)^2 \geq 0. \quad (10)$$

Note that

$$\frac{d\xi}{ds} \leq 0 \Leftrightarrow \frac{d\xi}{ds} = -\eta^{1/2}, \quad (11)$$

and that

$$\frac{d\xi}{ds} \geq 0 \Leftrightarrow \frac{d\xi}{ds} = \eta^{1/2}. \quad (12)$$

From Equation (9),

$$ds = \frac{d\xi}{\pm \sqrt{\eta}}. \quad (13)$$

Define, for convenience, a ‘‘shape kernel,’’

$$\theta = \pm \sqrt{\eta}, \quad (14)$$

where the sign is chosen from the physical considerations of Equations (11) and (12), such that

$$ds = \theta^{-1} d\xi. \quad (15)$$

(In particular, the upper sign applies when $\frac{d\xi}{ds} \geq 0$; the lower, when $\frac{d\xi}{ds} \leq 0$. This convention will be used throughout the remainder of the paper.) Equation (15) can be integrated to yield an expression for the umbilical length:

$$L = \int_0^L ds = - \int_{\xi_c}^{2\pi} \theta^{-1} d\xi. \quad (16)$$

From Equation (2),

$$dy = -s_\xi ds = -\theta^{-1} s_\xi d\xi, \quad (17)$$

such that

$$y = \int_\xi^{2\pi} \theta^{-1} s_\xi d\xi \left(= \pm \int_\xi^{2\pi} \eta^{-1/2} s_\xi d\xi \right) \quad (18)$$

and

$$y_c = \int_{\xi_c}^{2\pi} \theta^{-1} s_\xi d\xi \left(= \pm \int_{\xi_c}^{2\pi} \eta^{-1/2} s_\xi d\xi \right). \quad (19)$$

Likewise, Equation (3) yields

$$z = -\int_{\xi}^{2\pi} \theta^{-1} c_{\xi} d\xi \left(= \mp \int_{\xi}^{2\pi} \eta^{-1/2} c_{\xi} d\xi \right) \quad (20)$$

and

$$z_c = -\int_{\xi_c}^{2\pi} \theta^{-1} c_{\xi} d\xi \left(= \mp \int_{\xi_c}^{2\pi} \eta^{-1/2} c_{\xi} d\xi \right). \quad (21)$$

Together, Equations (16) and (18-21) describe the umbilical geometry as unique functions of the terminal angle ξ_c ; the terminal loads Q_y , Q_z , and M_x ; and the shape kernel θ .

VALIDATION (SPECIAL CASES)

The umbilical geometric equations, (16) and (18) through (21), can be used to derive equations for umbilical in-plane flexibilities. First, however, it will be shown as a check of the mathematics that the geometric equations simplify in some special cases to known forms [13].

Horizontal Cantilever with Vertical Point Load at Free End:

Consider the case where Q_y and M_x are both zero; this is Frisch-Fay's "basic strut" [13, p. 41].

Define, for convenience,

$$P_z = -Q_z. \quad (22)$$

Equation (16) becomes

$$L = \left(\frac{EI}{2P_z} \right)^{1/2} \int_{\xi_c}^{2\pi} (c_{\xi} - c_{\xi_c})^{-1/2} d\xi, \quad (23)$$

which can be rewritten as

$$L = \left(\frac{EI}{8P_z} \right)^{1/2} \int_{\xi_c}^{2\pi} \left(\sin^2 \frac{\xi_c}{2} - \sin^2 \frac{\xi}{2} \right)^{-1/2} d\xi. \quad (24)$$

Let

$$p \equiv \sin \frac{\xi_c}{2} \quad (25)$$

and select ϕ such that

$$p \sin \phi = \sin \frac{\xi}{2}. \quad (26)$$

Taking the differential of the above,

$$p \cos \phi d\phi = \frac{1}{2} \cos \frac{\xi}{2} d\xi. \quad (27)$$

From Equations (25) and (26),

$$\sin^2 \frac{\xi_c}{2} - \sin^2 \frac{\xi}{2} = p^2 (1 - \sin^2 \phi); \quad (28)$$

as ξ varies from ξ_c to 2π , ϕ varies from $\frac{\pi}{2}$ to π . In this range,

$$-\cos \phi = (1 - \sin^2 \phi)^{1/2} \quad (29)$$

and
$$-\cos \frac{\xi}{2} = (1 - p^2 \sin^2 \phi)^{1/2}, \quad (30)$$

so that
$$d\xi = \frac{-2p \cos \phi d\phi}{(1 - p^2 \sin^2 \phi)^{1/2}}. \quad (31)$$

Finally, using Equations (28) and (31) in Equation (24), and simplifying, one obtains the following result:

$$L = \frac{1}{k} K(p), \quad (32)$$

where
$$k^2 = \frac{P_z}{EI}, \quad (33)$$

and
$$K(p) = F(p, \pi/2) = \int_0^{\pi/2} (1 - p^2 \sin^2 \zeta)^{-1/2} d\zeta. \quad (34)$$

$K(p)$ and $F(p, \phi)$, respectively, are Legendre's complete and incomplete elliptic integrals of the 1st kind [13, p. 5]. Equation (32) is the solution previously reported in [13], page 41.

Horizontal Cantilever with Horizontal Point Load at Free End:

Consider next the case where Q_z and M_x are both zero. Equation (16) becomes

$$L = \left(\frac{EI}{2Q_y} \right)^{1/2} \int_{\xi_c}^{2\pi} (s_\xi - s_{\xi_c})^{-1/2} d\xi. \quad (35)$$

Introduce ϕ and positive parameter p such that $p^2 \equiv (1 - \sin \xi_c)/2$ (36)

and
$$\sin \phi \equiv \left(\frac{1 - \sin \xi}{2p^2} \right)^{1/2}. \quad (37)$$

Squaring the above yields
$$1 - \sin \xi = 2p^2 \sin^2 \phi. \quad (38)$$

Taking the differential,
$$\cos \xi d\xi = -4p^2 \sin \phi \cos \phi d\phi, \quad (39)$$

so that
$$d\xi = \frac{-4p^2 \sin \phi \cos \phi d\phi}{(1 - \sin^2 \xi)^{1/2}} d\phi. \quad (40)$$

From Equation (38) one obtains
$$1 + \sin \xi = 2(1 - p^2 \sin^2 \phi). \quad (41)$$

Equations (38) and (41) together yield

$$\left(1 - \sin^2 \xi\right)^{1/2} = 2p \sin \phi \left(1 - p^2 \sin^2 \phi\right)^{1/2}. \quad (42)$$

As ξ varies from ξ_c to 2π , ϕ varies from $\frac{\pi}{2}$ to $\sin^{-1} \frac{1}{p\sqrt{2}}$. Using Equation (42) in (40) yields

$$d\xi = \frac{-2p \cos \phi d\phi}{\left(1 - p^2 \sin^2 \phi\right)^{1/2}}. \quad (43)$$

Obtaining expressions for $\sin \xi_c$ and $\sin \xi$ from Equations (36) and (38), respectively, and substituting from these and Equation (40) into Equation (35), one obtains the following result:

$$L = \left(\frac{EI}{Q_y}\right)^{1/2} \int_m^{\pi/2} \left(1 - p^2 \sin^2 \phi\right)^{-1/2} d\phi, \quad (44)$$

where

$$m = \sin^{-1} \frac{1}{p\sqrt{2}}. \quad (45)$$

In terms of elliptic integrals,

$$L = \left(\frac{EI}{Q_y}\right)^{1/2} [K(p) - F(p, m)], \quad (46)$$

the solution previously reported in [13], page 42.

EQUATIONS OF UMBILICAL FLEXIBILITY

Nature of Dependencies on Flexural Rigidity EI

It will now be shown that, for constant values of L , ξ_c , y_c , and z_c , that is, umbilical length and terminal geometry, the following expressions are also constants: $\frac{Q_y}{EI}$, $\frac{Q_z}{EI}$, and $\frac{M_x}{EI}$. This will have important implications for umbilical shapes and flexibilities.

For convenience, define the following variables:

$$\alpha_1 = \frac{Q_y}{EI}, \quad (47)$$

$$\alpha_2 = \frac{Q_z}{EI}, \quad (48)$$

$$\alpha_3 = \frac{M_x}{EI} + \kappa_c^i, \quad (49)$$

$$\alpha_4 = \alpha_1 c_{\xi_c} + \alpha_2 s_{\xi_c}, \quad (50)$$

and

$$\alpha_5 = (\kappa^i)^2 - (\kappa_c^i)^2. \quad (51)$$

In the case of multiple umbilicals, let an additional subscript indicate the umbilical number: e.g., α_{ij} , θ_j , y_j , y_{cj} , ξ_{cj} . These symbols will be used in the subsequent development.

Consider now two umbilicals of uniform cross section, with identical lengths and terminal geometries, but different flexural rigidities EI and (thus) different (nonzero) terminal loads. In particular,

$$L_1 = L_2 = L > 0, \quad (52)$$

$$y_{c1} = y_{c2} = y_c, \quad (53)$$

$$z_{c1} = z_{c2} = z_c, \quad (54)$$

and

$$\xi_{c1} = \xi_{c2} = \xi_c, \quad (55)$$

but

$$(EI)_1 \neq (EI)_2. \quad (56)$$

Then

$$L_1 = -\int_{\xi_c}^{2\pi} \theta_1^{-1} d\xi = -\int_{\xi_c}^{2\pi} \theta_2^{-1} d\xi = L_2, \quad (57)$$

$$y_{c1} = \int_{\xi_c}^{2\pi} \theta_1^{-1} s_{\xi} d\xi = \int_{\xi_c}^{2\pi} \theta_2^{-1} s_{\xi} d\xi = y_{c2}, \quad (58)$$

and

$$z_{c1} = -\int_{\xi_c}^{2\pi} \theta_1^{-1} c_{\xi} d\xi = -\int_{\xi_c}^{2\pi} \theta_2^{-1} c_{\xi} d\xi = z_{c2}, \quad (59)$$

where

$$\theta_j(\xi_j) = \pm \left[2\alpha_{1j}(s_{\xi} - s_{\xi_c}) - 2\alpha_{2j}(c_{\xi} - c_{\xi_c}) + (\alpha_{3j}^2 + \alpha_{5j}) \right]^{1/2}. \quad (60)$$

From orthogonality of the constant (unity), sine, and cosine functions in Equations (57-59), respectively,

$$\theta_1 = \theta_2. \quad (61)$$

That is, with uniform cross sections and identical umbilical attachment angles,

$$\left. \begin{array}{l} L_1 = L_2 \\ y_{c1} = y_{c2} \\ z_{c1} = z_{c2} \end{array} \right\} \Rightarrow \theta_1 = \theta_2. \quad (62)$$

It can be shown by simple substitution that the “only if” statement of Equation (62) is, in fact, “if and only if” (\Leftrightarrow).

Using Equation (60), one can expand Equation (61) as follows:

$$\begin{aligned}\theta_1 &= \pm \sqrt{2\alpha_{11}(s_\xi - s_{\xi_c}) - 2\alpha_{21}(c_\xi - c_{\xi_c}) + (\alpha_{31}^2 + \alpha_{51})} \\ &= \pm \sqrt{2\alpha_{12}(s_\xi - s_{\xi_c}) - 2\alpha_{22}(c_\xi - c_{\xi_c}) + (\alpha_{32}^2 + \alpha_{52})} = \theta_2.\end{aligned}\quad (63)$$

Squaring and applying orthogonality as before, one concludes that

$$\theta_1 = \theta_2 \Rightarrow \begin{cases} \alpha_{11} = \alpha_{12} \\ \alpha_{21} = \alpha_{22} \\ \alpha_{31}^2 - \alpha_{51} = \alpha_{32}^2 - \alpha_{52} \end{cases} . \quad (64)$$

Again, it can be shown by simple substitution that this relationship is actually if and only if.

In summary,

$$\left. \begin{array}{l} L_1 = L_2 \\ y_{c1} = y_{c2} \\ z_{c1} = z_{c2} \end{array} \right\} \Leftrightarrow \theta_1 = \theta_2 \Leftrightarrow \begin{cases} \alpha_{11} = \alpha_{12} \\ \alpha_{21} = \alpha_{22} \\ \alpha_{31}^2 - \alpha_{51} = \alpha_{32}^2 - \alpha_{52} \end{cases} . \quad (65)$$

If the umbilicals also have identical initial curvatures, that is, for

$$\kappa_1^i(s) = \kappa_2^i(s) \quad \forall 0 \leq s \leq L, \quad (66)$$

one has that

$$\alpha_{51}(s) = \alpha_{52}(s), \quad (67)$$

such that

$$\left. \begin{array}{l} L_1 = L_2 \\ y_{c1} = y_{c2} \\ z_{c1} = z_{c2} \end{array} \right\} \Leftrightarrow \theta_1 = \theta_2 \Leftrightarrow \begin{cases} \alpha_{11} = \alpha_{12} \\ \alpha_{21} = \alpha_{22} \\ \alpha_{31} = \pm \alpha_{32} \end{cases} . \quad (68)$$

Equation (68) can be strengthened further as follows.

From Equation (7),

$$\alpha_3 = \frac{d\xi}{ds} \Big|_{R \rightarrow C} . \quad (69)$$

Also, from Equations (9) and (14),

$$\theta_1 = \theta_2 \Leftrightarrow \left(\frac{d\xi}{ds} \right)_1 = \left(\frac{d\xi}{ds} \right)_2 \quad \forall 0 \leq s \leq L . \quad (70)$$

Therefore, for $\theta_1 = \theta_2$, one can conclude that

$$\alpha_{31} = \pm \alpha_{32} \Leftrightarrow \alpha_{31} = \alpha_{32}, \quad (71)$$

In conclusion, if the two umbilicals have identical initial curvatures, Equation (65) reduces to the following:

$$\left. \begin{array}{l} L_1 = L_2 \\ y_{c1} = y_{c2} \\ z_{c1} = z_{c2} \end{array} \right\} \Leftrightarrow \theta_1 = \theta_2 \Leftrightarrow \begin{cases} \alpha_{11} = \alpha_{12} \\ \alpha_{21} = \alpha_{22} \\ \alpha_{31} = \alpha_{32} \end{cases} . \quad (72)$$

Equations (70) and (72) have the following physical significance: for a slender, terminally loaded umbilical (assuming only in-plane loading) that has a uniform cross section; a given, monotonically varying initial (i.e., relaxed) curvature; and a specified terminal geometry; changing the flexural rigidity by an arbitrary factor γ changes all terminal loads by the same factor without changing the umbilical shape. The implications for in-plane umbilical flexibilities will be explored in the next section.

FLEXIBILITY EQUATIONS

For a given terminal geometry (ξ_c , y_c , and z_c), one can now differentiate Equations (16), (19), and (21) with respect to the three terminal loads to yield expressions for the nine in-plane translational flexibilities. For convenience define the following “flexibility integrals”:

$$\beta_1 = \int_{\xi_c}^{2\pi} \theta^{-3} d\xi, \quad (73)$$

$$\beta_2 = \int_{\xi_c}^{2\pi} \theta^{-3} c_\xi d\xi, \quad (74)$$

$$\beta_3 = \int_{\xi_c}^{2\pi} \theta^{-3} s_\xi d\xi, \quad (75)$$

$$\beta_4 = \int_{\xi_c}^{2\pi} \theta^{-3} c_\xi^2 d\xi, \quad (76)$$

$$\beta_5 = \int_{\xi_c}^{2\pi} \theta^{-3} c_\xi s_\xi d\xi, \quad (77)$$

and

$$\beta_6 = \int_{\xi_c}^{2\pi} \theta^{-3} s_\xi^2 d\xi, \quad (78)$$

where, from Equations (10) and (14),

$$\theta = \pm \sqrt{2\alpha_1 (s_\xi - s_{\xi_c}) - 2\alpha_2 (c_\xi - c_{\xi_c}) + \alpha_3^2}. \quad (79)$$

According to Leibnitz' Rule,

$$\frac{\partial}{\partial x} \int_{f(x)}^{g(x)} F(x, \xi) d\xi = \int_{f(x)}^{g(x)} \frac{\partial}{\partial x} F(x, \xi) d\xi + F(x, g(x)) \frac{\partial g(x)}{\partial x} - F(x, f(x)) \frac{\partial f(x)}{\partial x}. \quad (80)$$

Applying Equation (80) to Equation (16), and substituting from Equations (47-51) and (73-78), one obtains the following expressions for the rotational flexibilities:

$$\frac{\partial \xi_c}{\partial Q_y} = \frac{\mp |\alpha_3|}{EI} \left[\frac{\beta_3 - s_{\xi_c} \beta_1}{1 \mp |\alpha_3| \alpha_4 \beta_1} \right], \quad (81)$$

$$\frac{\partial \xi_c}{\partial Q_z} = \frac{\pm |\alpha_3|}{EI} \left[\frac{\beta_2 - c_{\xi_c} \beta_1}{1 \mp |\alpha_3| \alpha_4 \beta_1} \right], \quad (82)$$

and

$$\frac{\partial \xi_c}{\partial M_x} = \frac{\mp |\alpha_3| \alpha_3}{EI} \left[\frac{\beta_1}{1 \mp |\alpha_3| \alpha_4 \beta_1} \right]. \quad (83)$$

Applying Leibnitz' Rule now to Equations (19) and (21), and substituting from Equations (81-83), one obtains the remaining six (translational) flexibility equations. The translational flexibilities are as follows:

$$\frac{\partial y_c}{\partial Q_y} = \frac{-1}{EI} \left[(\beta_6 - s_{\xi_c} \beta_3) - (\beta_3 - s_{\xi_c} \beta_1) \left(\frac{s_{\xi_c} \mp |\alpha_3| \alpha_4 \beta_3}{1 \mp |\alpha_3| \alpha_4 \beta_1} \right) \right], \quad (84)$$

$$\frac{\partial y_c}{\partial Q_z} = \frac{1}{EI} \left[(\beta_5 - c_{\xi_c} \beta_3) - (\beta_2 - c_{\xi_c} \beta_1) \left(\frac{s_{\xi_c} \mp |\alpha_3| \alpha_4 \beta_3}{1 \mp |\alpha_3| \alpha_4 \beta_1} \right) \right], \quad (85)$$

$$\frac{\partial y_c}{\partial M_x} = \frac{-\alpha_3}{EI} \left[\beta_3 - \beta_1 \left(\frac{s_{\xi_c} \mp |\alpha_3| \alpha_4 \beta_3}{1 \mp |\alpha_3| \alpha_4 \beta_1} \right) \right], \quad (86)$$

$$\frac{\partial z_c}{\partial Q_y} = \frac{1}{EI} \left[(\beta_5 - s_{\xi_c} \beta_2) - (\beta_3 - s_{\xi_c} \beta_1) \left(\frac{c_{\xi_c} \mp |\alpha_3| \alpha_4 \beta_2}{1 \mp |\alpha_3| \alpha_4 \beta_1} \right) \right], \quad (87)$$

$$\frac{\partial z_c}{\partial Q_z} = \frac{-1}{EI} \left[(\beta_4 - c_{\xi_c} \beta_2) - (\beta_2 - c_{\xi_c} \beta_1) \left(\frac{c_{\xi_c} \mp |\alpha_3| \alpha_4 \beta_2}{1 \mp |\alpha_3| \alpha_4 \beta_1} \right) \right], \quad (88)$$

and

$$\frac{\partial z_c}{\partial M_x} = \frac{\alpha_3}{EI} \left[\beta_2 - \beta_1 \left(\frac{c_{\xi_c} \mp |\alpha_3| \alpha_4 \beta_2}{1 \mp |\alpha_3| \alpha_4 \beta_1} \right) \right]. \quad (89)$$

An example derivation of a translational flexibility is provided in the Appendix.

END-STATE VERIFICATION

To verify the expressions for end-state geometry [i.e., Equations (16), (19), and (21)], a set of combined end-loads Q_y , Q_z , and M_x was initially selected, for an example umbilical, with the results to be compared to those of a corresponding finite-element simulation. The loads were then varied proportionally by use of a load-magnification factor λ to produce a family of loading conditions for comparison purposes.

The example umbilical has a rectangular cross-section, and forms a quarter circle of radius ρ in its relaxed configuration, with assigned values for ρ , for length L , and for flexural rigidity EI . The finite-element model comprises 40 equally-sized triangular shell elements composed of a linearly elastic material of assigned Young's modulus E , and Poisson's ratio ν . In particular, the selected

umbilical parameters are $\rho = 63.662 \text{ mm}$, $L = 100 \text{ mm}$, $EI = 1250 \text{ N}\cdot\text{mm}^2$, $E = 7.5 \cdot 10^{12} \text{ N/m}^2$, and $\nu = 0.28$. Its cross-sectional width is 2mm; and its height (i.e., shell thickness), 0.1 mm. The assigned end-loads are $Q_y = 0.01\lambda \text{ N}$, $Q_z = -0.01\lambda \text{ N}$, and $M_x = -25\lambda \text{ N}\cdot\text{mm}$, where λ varies from 0.01 to 1.0, in increments of 0.01.

Calculations were made of the terminal geometry (y_c, z_c, ξ_c) , from the analytical expressions [Eqs. (16), (19), and (21)], for each value of λ , using an iterative process in which an initial guess was made for the end-angle ξ_c , followed by formation of the shape kernel θ [Eqs. (10) and (14)], and by calculation of the resulting length L [using a numerical approximation of Equation (16)]. Based on the error in L , a new estimate for ξ_c was determined by adding an amount proportional to the calculated error. The iterations were continued until the percent error calculated for L was less than $1.0 \cdot 10^{-7}$. After convergence, the end coordinates (y_c, z_c) were calculated using Equations (19) and (21). The resulting terminal geometry is presented in Figure 2a, as a function of λ , by solid lines.

The finite element model was then used to verify the terminal geometry calculated above, by determining the end coordinates (y_c, z_c) for the various values of λ . The results are shown as markers in Figure 2a. The results from the analytical model (solid lines) and those from the finite-element model were found to be in excellent agreement. Figure 3 shows the initial and final configurations of the example umbilical, for $\lambda = 1$.

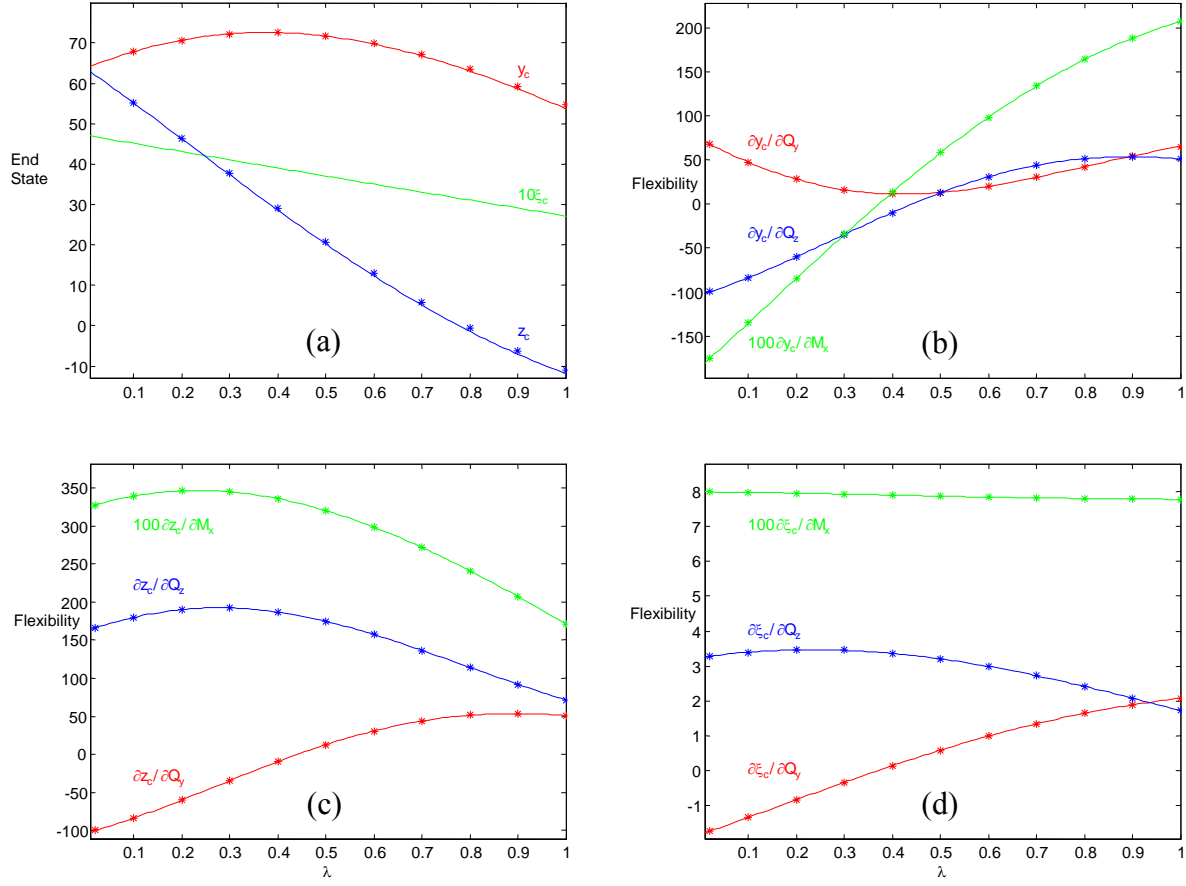


Figure 2: End-state and flexibilities versus load factor λ for curved ($1/4$ -circle) umbilicals with flexural rigidity $EI=1250\text{N}\cdot\text{mm}^2$, length $L=100\text{mm}$, radius of curvature $\rho = 63.662\text{ mm}$ (curvature $\kappa^i = -0.01571\text{mm}^{-1}$), and end-loadings $Q_y = 0.01\lambda\text{ N}$, $Q_z = -0.01\lambda\text{ N}$, and $M_x = -25\lambda\text{ N}\cdot\text{mm}$, where λ varies from 0.01 to 1.0 in increments of 0.01. Solid lines denote results calculated using the analytical expressions; markers denote results calculated using either the finite-element model (a) or finite-difference approximations (b, c, and d).

FLEXIBILITY VERIFICATION

Once the end-states had been verified, they could be used in turn to verify the flexibility equations [Eqs. (81) through (89)], by finite difference approximations. The pertinent finite difference approximations follow:

$$\frac{\partial y_c}{\partial Q_y} = \frac{y_c|_{Q_y+\Delta Q_y, Q_z, M_x} - y_c|_{Q_y, Q_z, M_x}}{\Delta Q_y} + \text{oh}(2), \quad (90)$$

$$\frac{\partial y_c}{\partial Q_z} = \frac{y_c|_{Q_y, Q_z+\Delta Q_z, M_x} - y_c|_{Q_y, Q_z, M_x}}{\Delta Q_z} + \text{oh}(2), \quad (91)$$

$$\frac{\partial y_c}{\partial M_x} = \frac{y_c |_{Q_y, Q_z, M_x + \Delta M_x} - y_c |_{Q_y, Q_z, M_x}}{\Delta M_x} + \text{oh}(2), \quad (92)$$

$$\frac{\partial z_c}{\partial Q_y} = \frac{z_c |_{Q_y + \Delta Q_y, Q_z, M_x} - z_c |_{Q_y, Q_z, M_x}}{\Delta Q_y} + \text{oh}(2), \quad (93)$$

$$\frac{\partial z_c}{\partial Q_z} = \frac{z_c |_{Q_y, Q_z + \Delta Q_z, M_x} - z_c |_{Q_y, Q_z, M_x}}{\Delta Q_z} + \text{oh}(2), \quad (94)$$

$$\frac{\partial z_c}{\partial M_x} = \frac{z_c |_{Q_y, Q_z, M_x + \Delta M_x} - z_c |_{Q_y, Q_z, M_x}}{\Delta M_x} + \text{oh}(2), \quad (95)$$

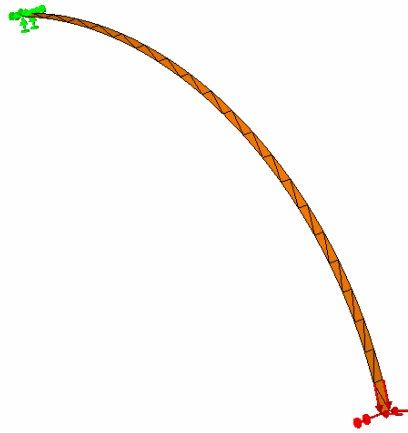
$$\frac{\partial \xi_c}{\partial Q_y} = \frac{\xi_c |_{Q_y + \Delta Q_y, Q_z, M_x} - \xi_c |_{Q_y, Q_z, M_x}}{\Delta Q_y} + \text{oh}(2), \quad (96)$$

$$\frac{\partial \xi_c}{\partial Q_z} = \frac{\xi_c |_{Q_y, Q_z + \Delta Q_z, M_x} - \xi_c |_{Q_y, Q_z, M_x}}{\Delta Q_z} + \text{oh}(2), \quad (97)$$

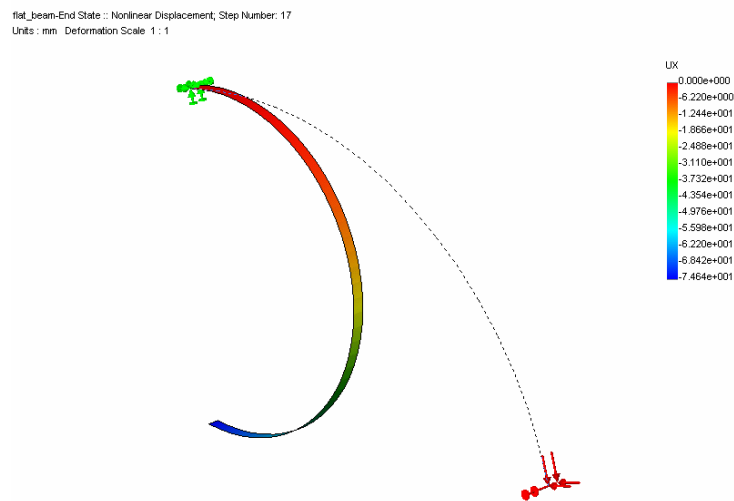
and

$$\frac{\partial \xi_c}{\partial M_x} = \frac{\xi_c |_{Q_y, Q_z, M_x + \Delta M_x} - \xi_c |_{Q_y, Q_z, M_x}}{\Delta M_x} + \text{oh}(2). \quad (98)$$

The finite-difference approximations to the flexibilities [Eqs. (90) through (98)] were calculated over the selected range of values for λ , using the verified end-states that had been calculated previously. The value chosen for each of the increments ΔQ_y , ΔQ_z , and ΔM_x corresponds to a 0.01% change from the respective nominal value. Finite-difference results for the flexibilities are shown as markers in Figures 2b, c, and d. The analytical models (shown by solid lines) are seen to be in excellent agreement with the finite-difference calculations.



[a]



[b]

Figure 3: Finite-element model of the example umbilical defined in the caption of Fig. 2. The physical umbilical modeled has a rectangular cross-section of width 2mm and height (i.e. shell thickness) of 0.1mm. The finite-element discretization comprises 40 equally-sized triangular shell elements composed of a linearly elastic material, defined by Young's modulus $E = 7.5E+12$ N/m² and Poisson's ratio $\nu = 0.28$. The resulting EI of the model equals 1250 N-mm², as required. Shown is the model in its undeformed state (a) and deformed state (b), after a loading corresponding to $\lambda = 1.0$. The analysis was carried out using the nonlinear solver incorporated into the commercial package COSMOS/DesignStar.

IMPLICATIONS FOR UMBILICAL DESIGN

The foregoing equations can be used as an aid for designing umbilicals to minimize stiffness. First, the flexural rigidity can be used to adjust all stiffnesses by a common factor. Since all of the α_i 's and β_i 's are invariant with flexural rigidity, the square-bracketed factors of the flexibility equations, Equations (56) through (64), are all independent of flexural rigidity. It is evident from these equations, then, that reductions in EI will produce proportional reductions in all terminal loads and in-plane stiffnesses. Second, for given umbilical length L , and endpoint conditions ξ_c , y_c , and z_c , Equations (16), (19), and (21) can be solved for the loads Q_y , Q_z , and M_x . These loads can be determined and used iteratively in the flexibility equations to optimize the umbilical flexibilities (or, equivalently, the corresponding stiffnesses) using L as a parameter. Third, the umbilical designer can use these equations to determine optimal L , ξ_c combinations. Although the angle ξ_c is fixed at about 225 deg for ARIS (in the home, or centered, position); L and ξ_c optimization could suggest better angles for future designs.

CONCLUSION

This research has presented equations for the shape and flexibilities of a slender umbilical on orbit, that is, such that gravity can be neglected, under general, terminal, in-plane loading conditions of sufficient magnitude to cause large deformations. The relaxed (preloaded) umbilical was assumed to be curved, with monotonically varying slope, and to have a uniform cross section. The loaded umbilical is assumed to undergo no plastic deformation. All in-plane stiffnesses were shown to be proportional to the flexural rigidity EI . The geometric end-state equations and umbilical flexibility expressions were verified numerically for an initially circular umbilical, subject to in-plane end-loading conditions. An approach was offered for using umbilical length and terminal geometry (endpoint locations and slopes) to optimize these umbilical stiffnesses. The basic geometric equations for an initially straight cantilever were shown to reduce to previously published results for special loading conditions.

APPENDIX: SAMPLE DERIVATION OF A FLEXIBILITY EQUATION

From Equation (19), the y -coordinate of terminal point C is

$$y_c = \int_{\xi_c}^{2\pi} \theta^{-1} s_\xi d\xi, \quad (19, A-1)$$

where

$$\theta(\xi) = \pm \left[2\alpha_1 (s_\xi - s_{\xi_c}) - 2\alpha_2 (c_\xi - c_{\xi_c}) + (\alpha_3^2 + \alpha_5) \right]^{1/2}, \quad (60, A-2)$$

for

$$\alpha_1 = \frac{Q_y}{EI}, \quad (47, A-3)$$

$$\alpha_2 = \frac{Q_z}{EI}, \quad (48, A-4)$$

$$\alpha_3 = \frac{M_x}{EI} + \kappa_c^i, \quad (49, A-5)$$

and

$$\alpha_5 = (\kappa^i)^2 - (\kappa_c^i)^2. \quad (51, A-6)$$

Taking the partial derivative of Equation (A-1) with respect to Q_y , one has

$$\frac{\partial y_c}{\partial Q_y} = \frac{\partial}{\partial Q_y} \left(\int_{\xi_c}^{2\pi} \theta^{-1} s_\xi d\xi \right). \quad (A-7)$$

Applying Leibnitz' Rule,

$$\frac{\partial y_c}{\partial Q_y} = \int_{\xi_c}^{2\pi} \frac{\partial}{\partial Q_y} (\theta^{-1} s_\xi) d\xi + (\theta^{-1} s_\xi) \Big|_{\xi \rightarrow 2\pi} \frac{\partial (2\pi)}{\partial Q_y} - (\theta^{-1} s_\xi) \Big|_{\xi \rightarrow \xi_c} \frac{\partial \xi_c}{\partial Q_y}. \quad (A-8)$$

The right-hand side of this equation will next be evaluated term by term.

The integrand of the first right-hand-side term is

$$\frac{\partial}{\partial Q_y} (\theta^{-1} s_\xi) = -s_\xi \theta^{-3} \left[\frac{1}{EI} (s_\xi - s_{\xi_c}) - (\alpha_1 c_{\xi_c} + \alpha_2 s_{\xi_c}) \frac{\partial \xi_c}{\partial Q_y} \right], \quad (A-9)$$

so that the integral itself becomes

$$\int_{\xi_c}^{2\pi} \frac{\partial}{\partial Q_y} (\theta^{-1} s_\xi) d\xi = \frac{-1}{EI} \left(\int_{\xi_c}^{2\pi} s_\xi^2 \theta^{-3} d\xi - s_{\xi_c} \int_{\xi_c}^{2\pi} s_\xi \theta^{-3} d\xi \right) + (\alpha_1 c_{\xi_c} + \alpha_2 s_{\xi_c}) \int_{\xi_c}^{2\pi} s_\xi \theta^{-3} d\xi \frac{\partial \xi_c}{\partial Q_y}. \quad (A-10)$$

The second right-hand-side term of Equation (A-8) is zero, since 2π is a constant.

The third right-hand-side term is

$$-\left(\theta^{-1}s_{\xi}\right)_{\xi \rightarrow \xi_c} \frac{\partial \xi_c}{\partial Q_y} = -\left(\pm |\alpha_3|^{-1} s_{\xi_c}\right) \frac{\partial \xi_c}{\partial Q_y}, \quad (\text{A-11})$$

where the sign accompanying $|\alpha_3|^{-1}$ is that of slope $d\xi/ds$. By similar application of Leibnitz' Rule to the equation

$$L = -\int_{\xi_c}^{2\pi} \theta^{-1} d\xi, \quad (\text{16, A-12})$$

one has

$$\frac{\partial \xi_c}{\partial Q_y} = \frac{\mp |\alpha_3|}{EI} \left[\frac{\int_{\xi_c}^{2\pi} \theta^{-3} s_{\xi} d\xi - s_{\xi_c} \int_{\xi_c}^{2\pi} \theta^{-3} d\xi}{1 \mp |\alpha_3| \alpha_4 \int_{\xi_c}^{2\pi} \theta^{-3} d\xi} \right]. \quad (\text{A-13})$$

Substituting from Equations (A-9), (A-11), and (A-13) into Equation (A-8), and using Equations (73), (75), (78) to re-express the result in terms of the β_i 's, one obtains the form given in Equation (84):

$$\frac{\partial y_c}{\partial Q_y} = \frac{-1}{EI} \left[(\beta_6 - s_{\xi_c} \beta_3) - (\beta_3 - s_{\xi_c} \beta_1) \left(\frac{s_{\xi_c} \mp |\alpha_3| \alpha_4 \beta_3}{1 \mp |\alpha_3| \alpha_4 \beta_1} \right) \right]. \quad (\text{84, A-14})$$

The other flexibility equations can be determined analogously.

REFERENCES

- ¹Edberg, D. L., and Wilson, B. W., "Design and Testing of Reduced-Stiffness Umbilicals for Space Station Microgravity Isolation," AIAA Paper 2000-1408, April 2000.
- ²Hummel, F. H., and Morton, W. B., "On the Large Deflection of Thin Flexible Strips and the Measurement of Their Elasticity," *Philosophical Magazine*, Ser. 7, Vol. 17, 1927, pp. 348-357.
- ³Gross, S., and Lehr, E., *Die Federn*, V. D. I. Verlag, Berlin, Germany, 1938.
- ⁴Barten, H. J., "On the Deflection of a Cantilever Beam," *Quarterly of Applied Mathematics*, Vol. 2 (2), 1944, pp. 168-171.
- ⁵Barten, H. J., "On the Deflection of a Cantilever Beam," *Quarterly of Applied Mathematics*, Vol. 3 (3), 1945, pp. 275, 276.
- ⁶Bisshopp, K. E., and Drucker, D. C., "Large Deflections of Cantilever Beams," *Quarterly of Applied Mathematics*, Vol. 3 (3), Oct. 1945, pp. 272-275.
- ⁷Bickley, W. G., "The Heavy Elastica," *Philosophical Magazine*, Ser. 7, Vol. 17, 1934, pp. 603-622.
- ⁸Rohde, F. V., "Large Deflections of a Cantilever Beam with a Uniformly Distributed Load," *Quarterly of Applied Mathematics*, Vol. 11, 1953, pp. 337, 338.
- ⁹Schmidt, R., and Dadeppo, D. A., "Large Deflections of Heavy Cantilever Beams and Columns," *Quarterly of Applied Mathematics*, Oct. 1970, 441-444.
- ¹⁰Mitchell, T. P., "The Non-Linear Bending of Thin Rods," *Journal of Applied Mechanics*, Vol. 26, 1959, pp. 40-43.
- ¹¹Beth, R. A., and Wells, C. P., "Finite Deflections of a Cantilever Strut," *Journal of Applied Physics*, Vol. 22, 1951, pp. 742-746.
- ¹²Massoud, M. F., "On the Problem of Large Deflection of a Cantilever Beam," *International Journal of Mechanical Sciences*, Vol. 8, Feb. 1966, pp. 141-143.
- ¹³Frisch-Fay, R., *Flexible Bars*, Butterworths, London, 1962, pp. 5, 42.
- ¹⁴Antman, S. S., Marlow, R. S., and Vlahacos, C. P., "The Complicated Dynamics of Heavy Rigid Bodies Attached to Deformable Rods," *Quarterly of Applied Mathematics*, Vol. 56, No. 3, Sep. 1998, pp. 431-460.
- ¹⁵Manuel, F. S., and Lee, S. L., "Flexible Bars Subjected to Arbitrary Discrete Loads and Boundary Conditions," *Journal of the Franklin Institute*, Vol. 285 (6), 1968, pp. 452-474.
- ¹⁶Rojahn, C., "Large Deflections of Elastic Beams," Degree of Engineer Thesis, Stanford University, June 1968.
- ¹⁷Gorski, W., "A Review of the Literature and a Bibliography on Finite Elastic Deflections of Bars," *Institute of Engineers, Australia: Civil Engineering Transactions*, Vol. CE18, 1976, pp. 74-85.

¹⁸Libai, A., and Simmonds, J. G., *The Nonlinear Theory of Elastic Shells*, 2nd ed., Cambridge Univ. Press, Cambridge, England, U.K., 1998.

¹⁹Hampton, R. D., Quraishi, N., and Rupert, J. K., "Flexibility Equations for Active Rack Isolation System Umbilicals with Planar End Loading (TN)," *AIAA Journal*, Vol. 39 (10), Oct. 2001, pp. 2024-2027.

REPORT DOCUMENTATION PAGE			Form Approved OMB No. 0704-0188	
Public reporting burden for this collection of information is estimated to average 1 hour per response, including the time for reviewing instructions, searching existing data sources, gathering and maintaining the data needed, and completing and reviewing the collection of information. Send comments regarding this burden estimate or any other aspect of this collection of information, including suggestions for reducing this burden, to Washington Headquarters Services, Directorate for Information Operations and Reports, 1215 Jefferson Davis Highway, Suite 1204, Arlington, VA 22202-4302, and to the Office of Management and Budget, Paperwork Reduction Project (0704-0188), Washington, DC 20503.				
1. AGENCY USE ONLY (Leave Blank)	2. REPORT DATE January 2005	3. REPORT TYPE AND DATES COVERED NASA Technical Manual		
4. TITLE AND SUBTITLE Deformation and Flexibility Equations for ARIS Umbilicals Idealized as Planar Elastica			5. FUNDING NUMBERS	
6. AUTHOR(S) R. David Hampton, Michael J. Leamy, Paul J. Bryant, Naveed Quraishi				
7. PERFORMING ORGANIZATION NAME(S) AND ADDRESS(ES) Lyndon B. Johnson Space Center Houston, Texas 77058			8. PERFORMING ORGANIZATION REPORT NUMBERS S-948	
9. SPONSORING/MONITORING AGENCY NAME(S) AND ADDRESS(ES) National Aeronautics and Space Administration Washington, DC 20546-0001			10. SPONSORING/MONITORING AGENCY REPORT NUMBER TM-2004-213155	
11. SUPPLEMENTARY NOTES				
12a. DISTRIBUTION/AVAILABILITY STATEMENT Category: 67 Available from the NASA Center for AeroSpace Information (CASI) 7121 Standard Hanover, MD 21076-1320			12b. DISTRIBUTION CODE	
13. ABSTRACT (Maximum 200 words) The International Space Station relies on the active rack isolation system (ARIS) as the central component of an integrated, station-wide strategy to isolate microgravity space-science experiments. ARIS uses electromechanical actuators to isolate an international standard payload rack from disturbances due to the motion of the Space Station. Disturbances to microgravity experiments on ARIS-isolated racks are transmitted primarily via the ARIS power and vacuum umbilicals. Experimental tests indicate that these umbilicals resonate at frequencies outside the ARIS controller's bandwidth at levels of potential concern for certain microgravity experiments. Reduction in the umbilical resonant frequencies could help to address this issue. This work documents the development and verification of equations for the in-plane deflections and flexibilities of an idealized umbilical (thin, flexible, inextensible, cantilever beam) under end-point, in-plane loading (inclined-force and moment). The effect of gravity is neglected due to the on-orbit application. The analysis assumes an initially curved (not necessarily circular), cantilevered umbilical with uniform cross-section, which undergoes large deflections with no plastic deformation, such that the umbilical slope changes monotonically. The treatment is applicable to the ARIS power and vacuum umbilicals under the indicated assumptions.				
14. SUBJECT TERMS ISS, Space Station, ARIS, microgravity, umbilicals, planar elastica			15. NUMBER OF PAGES 20	16. PRICE CODE
17. SECURITY CLASSIFICATION OF REPORT Unclassified	18. SECURITY CLASSIFICATION OF THIS PAGE Unclassified	19. SECURITY CLASSIFICATION OF ABSTRACT Unclassified	20. LIMITATION OF ABSTRACT Unlimited	